applied sciences

MDPI

Article

Use of Raman Spectroscopy, Scanning Electron Microscopy and Energy Dispersive X-ray Spectroscopy in a Multi-Technique Approach for Physical Characterization of Purple Urine Bag Syndrome

Giuseppe Acri [1], Carlo Sansotta [1,*], Francesca Maria Salmeri [1], Marco Romeo [2], Elisa V. Ruello [1], Lucia Denaro [1] and Barbara Testagrossa [1]

[1] Department of Biomedical and Dental Science and Morphofunctional Imaging, Messina University, 98122 Messina, Italy; giuseppe.acri@unime.it (G.A.); francescamaria.salmeri@unime.it (F.M.S.); elisa.ruello@unime.it (E.V.R.); lucia.denaro@unime.it (L.D.); barbara.testagrossa@unime.it (B.T.)
[2] Carabinieri Department Forensic Science Investigations, 98121 Messina, Italy; marco.b.romeo@gmail.com
* Correspondence: sansotta@unime.it

Abstract: Purple urine bag syndrome (PUBS) is a rare condition characterized by purple discoloration of urine and urine bags. Although it is benign, it represents an alarming symptom to the patients and their relatives because of purple discoloration. We have physically characterized urine and urine bags belonging to a patient suffering from PUBS using an approach that combines Raman spectroscopy (RS) and scanning electron microscopy (SEM) coupled with energy dispersive X-ray (EDX). Five "blue" discolored bags and one sterile urine bag, representing the control, were cut into 1 cm^2 square samples and analyzed by using RS and SEM + EDX technique. RS enabled us to identify the presence of indigo, a metabolite of tryptophan, while SEM analysis showed the biofilm deposit, probably due to the presence of microorganisms, and the EDX measurements exhibited the elemental composition of the bags. In particular, urine bags before and after the presence of PUBS urine showed an increase of ~32% of Cl, ~33% of O, ~667% of Ca, ~65% of Al and Mg, while C decreased by about 41%. Our results, to be taken as a proof-of-principle study, are promising for the aim to characterizing the urine bags in a flexible, inexpensive, and comprehensive manner.

Keywords: multi-technique; spectrometers; RS; SEM; EDX; PUBS

Citation: Acri, G.; Sansotta, C.; Salmeri, F.M.; Romeo, M.; Ruello, E.V.; Denaro, L.; Testagrossa, B. Use of Raman Spectroscopy, Scanning Electron Microscopy and Energy Dispersive X-ray Spectroscopy in a Multi-Technique Approach for Physical Characterization of Purple Urine Bag Syndrome. *Appl. Sci.* **2022**, *12*, 4034. https://doi.org/10.3390/app12084034

Academic Editor: Thomas Schmid

Received: 22 February 2022
Accepted: 15 April 2022
Published: 16 April 2022

1. Introduction

Purple urine bag syndrome (PUBS) is a rare, uncommon condition that occurs in chronic urinary catheterized patients with urinary tract infection [1,2]. It is characterized by the blue/purple discoloration of a catheter and of a Foley bag over hours to days [2,3]. The change in color actually occurs within the urine bag, whereas, interestingly, the urine remains unchanged in color [4]. It is considered a benign condition that requires no treatment other than changing the Foley bag, although antibiotics are occasionally used [2]. However, this condition is worrisome to and causes distress among patients, caregivers, and healthcare providers due to the clearly alarming urine and bag color [5]. PUBS is associated in patients with debilitation, renal failure, bacteriuria, alkaline urine, an indwelling urinary catheter, and chronic constipation [1,2,6]. The majority of patients suffering from PUBS are catheterized due to significant disability, typically being chair-bound or bed-bound elderly patients [1].

Raman Spectroscopy (RS), belonging to the family of vibrational spectroscopic techniques, is a powerful spectroscopic modality that relies on the inelastic scattering process of monochromatic light, such as laser light [7]. The Raman spectra exhibit spectral features that are characteristic for molecular structure and conformation, giving a molecular fingerprint of the sample. RS represents an essential methodology in different research

fields, such as chemistry, physics, biology, and material sciences [8–11], and its advanced applications are currently employed in the biomedical field and many applications were reported [12–15]. As RS is a rapid and nondestructive analysis technique for the detection of biochemical changes at the molecular level and does not require any preparation before the measurement, RS can be used for in vitro and in vivo measurements of analytes in biological fluids in their native liquid state [16,17].

RS, for instance, may apply to analyze the urine, a body fluid providing information about the body's metabolism and renal function. Urinalysis, including physical, chemical, and microscopic examinations, is an important laboratory test that is especially helpful in the diagnosis of urinary tract diseases. RS can be useful to detect various metabolites such as urea and uric acid, creatinine, ketone bodies (hydroxybutyrate and acetoacetate), phosphate, and other nitrogen compounds in urine, many of which are intrinsic native fluorophores [18]. Changes in these components reflect the metabolism of the human body and depend on the different kinds of food intake [19], or may be due to pathological conditions. Therefore, this information may be correlated with clinical criteria for the diagnosis of various renal, metabolic, and systemic diseases [16,20,21].

In addition, scanning electron microscopy (SEM) analysis has been performed to morphologically characterize the sample under investigation. The SEM analysis has been coupled with energy dispersive X-ray spectroscopy (EDX) microanalysis to determine the elemental composition of the sample surface. The combination of these techniques has a wide range of applications in various industrial, commercial, and research fields [22,23]. These practices are applied in the morpho-compositional analysis of urinary stones [24], but their application in the area of microbial detection is rare [25], whereas SEM plays a crucial role in detecting the cause of infection and disease [26].

We have not found studies concerning the RS and/or SEM or SEM + EDX characterization of urine and urine bags obtained from PUBS subjects in the literature, even if many clinical cases are reported. Therefore, the aim of the study was to physically characterize urine and urine bag samples of a woman affected by multiple pathologic conditions with an apparent discoloration of the urine collected in the urine bags using these techniques.

2. Materials and Methods

A 57-year-old woman was attending our unit at the University of Messina, Italy, on January 2021 because her husband's observation of seemingly blue discoloration of the urine catheter and urine bag which occurred every time a few days after the silicon catheter change, apart from the first three changes. The medical history of our patient is very complicated because she was suffering from various pathologies. See in the Supplementary Materials for the comprehensive medical history and clinical data of the patient.

Urine specimens from both the patient's renal pelvis and urine bag were collected in sterile containers in the morning and analyzed at room temperature within 1 h of collection to avoid changes, such as an increase in pH (due to breakdown of urea to ammonia), a decrease in bilirubin (due to light exposure), and changes in color (due to oxidation or reduction reactions). Urine specimens were neither treated nor processed. All urine specimens were analyzed by using RS.

Sterile urine bags were used to collect the patient's urine. The bags, with a capacity of 2000 mL, and the tubes are made of polyvinyl chloride (PVC). PVC is a synthetic thermoplastic material, chemically nonreactive, obtained by polymerization of vinyl chloride monomers. Sterility inside the bags is maintained by the presence of a nonreturn valve that prevents urine back flow into the indwelling urinary catheter.

Five "blue" discolored bags and one sterile urine bag, as a control, were cut into 1 cm^2 square samples, using a sterile scissor. All samples were analyzed by using SEM + EDX.

Raman measurements were performed by using a DXR-SmartRaman Spectrometer (Thermo Fisher Scientific, Waltham, MA, USA). The experimental setup was equipped with 180-degree sampling accessory. The spectra were acquired using a diode laser source with the excitation wavelength of 780 nm. All Raman spectra were acquired over the wavenum-

ber range of 3300–200 cm^{-1} with an estimated resolution between 4.7 and 8.8 cm^{-1}, and irradiated with a laser power of 24 mW, coming out from a 50-µm spot (estimated spot size 3.1 µm). The estimated data spacing was 1.9285 cm^{-1}. To obtain high signal-to-noise ratio (S/R) spectra, the Raman spectrum of each sample was obtained in triplicate after collecting 32 sample exposures for each spectrum, and the duration of each exposure during data collection was set equal to 60.0 s. Total acquisition time was 32 min for each spectrum. All Raman spectra were corrected for fluorescence by subtracting a fifth-order polynomial via a least squares fit, and also for cosmic ray artifacts. All Raman spectra were stored in .spa format, and the post-processing analyses were performed by using the Omnic For Dispersive Raman version 9.1.24 software (Thermo Fisher Scientific Madison, WI, USA). When the acquisition of the Raman spectra was complete, the average spectrum for each sample was calculated, and a baseline subtraction was applied (polynomial spline) to a manually chosen point in the wavenumber range 300–2000 cm^{-1}.

Each 1-cm^2 square bag sample was mounted on an adhesive black carbon tab, pre-mounted on the sample holder, and then analyzed by an FEI Quanta 450 FEG Thermofisher Scientific Scanning Electron Microscope to evaluate its morphological characteristics. This is a field emission gun—scanning electron microscope (FEG-SEM) used for high-resolution imaging (morphological and compositional) of both conductive and non-conductive specimens at the nanometer-scale resolution and for semi-quantitative X-ray microanalysis. We used it in the "low vacuum mode" (LV), where electrically non-conductive samples can be imaged without the need of a conductive layer (e.g., carbon, gold etc.). Each sample surface was scanned in the X-Y direction using the electron beam generated by the electron gun. The SEM measurements were conducted at 25.5 kV. We used magnification of ×720, ×1200 and ×1500, then we discarded the observations at ×1200 and retained the ×720 and ×1500 ones. The images were obtained in back-scattered electron (BSE) mode. The working distance (WD) was between 13.5 and 13.8 mm. The series of images we have obtained were then saved on the local hard-disk of the PC in .tiff format at 16 bit and were not elaborated in any way.

The elemental analysis of the drainage bag was performed by the EDX of the FEI Quanta 450 FEG. As a result, an X-ray spectrum was obtained and the instrumentation gave us the elemental composition, with relative errors, in percentages as a table. In the spectrum, the peak position identifies the different elements in the sample surface, whereas its intensity allows quantitative characterization of each detected element. The analysis results were carried out according to the reference energy spectrum of the calibration included in the instrument library. Both qualitative and quantitative elemental analyses were conducted at four different points on each sample surface. The obtained results represent the mean value of four different measurements effectuated on every target sample.

3. Results

Urine specimens collected both from the renal pelvis and from drainage "blue" bags revealed no color alteration, nor differences in coloration.

The difference between the average Raman spectrum of the urine sample collected from the renal pelvis and the average Raman spectrum of the sample collected from the drainage urinary bag was calculated to remove the spectral features of urine from the spectrum of a mixture of compounds. The difference spectrum has been baselined. The resulting Raman spectra are shown in Figure 1.

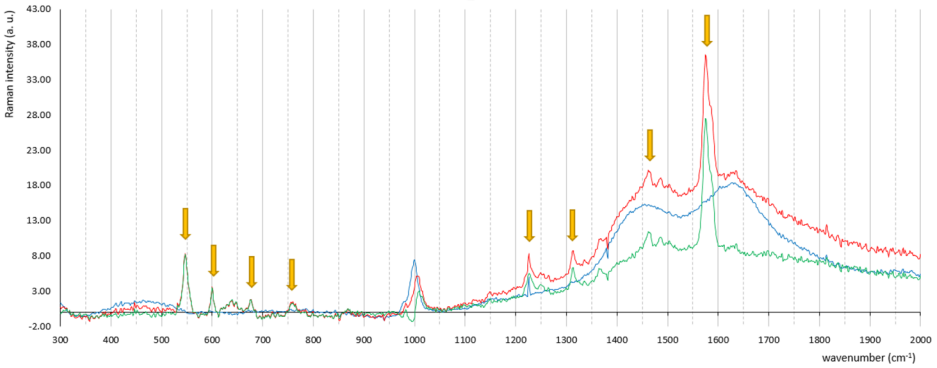

Figure 1. Average spectrum of the patient urine specimens from the renal pelvis (red line), from the drainage "blue" bag (blue line) and the difference spectrum between them (green line). Yellow arrows point out peaks located at 546 cm^{-1}, 600 cm^{-1}, 676 cm^{-1}, 759 cm^{-1}, 1226 cm^{-1}, 1313 cm^{-1}, 1461 cm^{-1}, and 1573 cm^{-1} in the urine from the renal pelvis spectrum that are not present in the urine from drainage "blue" bag spectrum.

The profile of the final spectrum (the green line in Figure 1) reveals the presence of indigo and the experimental vibrational peaks with their tentative assignments are detailed in Table 1. In the same table, based on literature, the vibrational peaks of a pilot study [27] are also reported.

Table 1. Experimental vibrational peaks with their tentative assignments, based on literature. Legend for intensity: vw = very weak; w = weak; m = medium; s = strong; vs = very strong.

Experimental Peaks (cm^{-1})	Ref Peaks (cm^{-1}) [25]	Intensity	Assignment
469.2	467	vw	γ C-C
546.7	544	m	δ C=C-CO-C
600.0	598	vw	δ C=O δ C-H δ C-NH-C
639.6	635	w	γ N-H
676.3	674	vw	δ C-C
759.5	758	vw	δ C-H δ N-C-C
867.9	868	vw	ν C-N
948.9	940	vw	γ C-H
1008.8	1015	m	δ C-H
1149.1	1147	vw	δ C-C
1226.2	1224	s	δ C-H ν C-N
1248.9	1248	m	δ C-H δ C=O
1312.7	1310	s	ν C-C
1364.6	1365	s	δ N-H δ C-H
1461.8	1460	s	ν C-C δ C-H
1486.2	1482	s	ν C-C δ C-H
1575.1	1582	vs	ν C=C ν C=O
1624.4	1625	s	ν C-C δ C-H
1697.9	1701	w	ν C=C ν C=O

Typical morphological images obtained using a SEM technique from the control urine bag and the "blue" one are displayed in Figure 2, whereas a thick biofilm of the deposited material covers the surface of the "blue" bag in the right side of the figure.

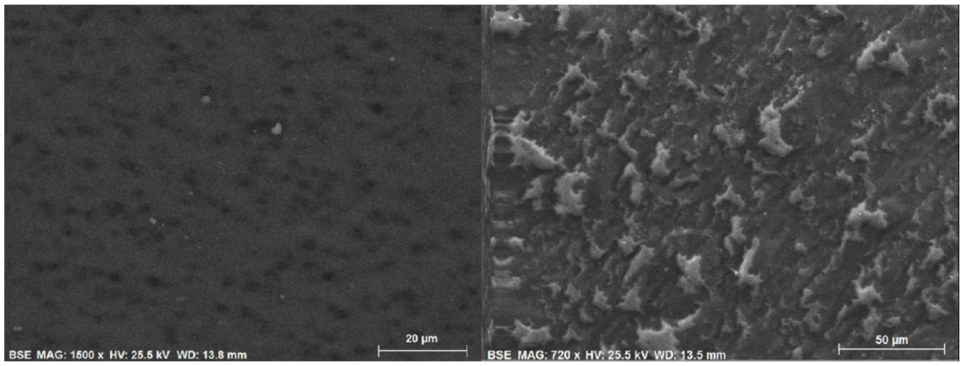

Figure 2. Morphological images of urine drainage bag obtained using the scanning electron microscope. On the left side, the clean bag (control); on the right side, the "blue" bag.

The EDX analysis was applied to detect the elemental composition of the bag both before (control) and after the use by the patient ("blue bags"). The results of the EDX analysis are reported in Table 2. EDX provides elemental data in both atomic and weight percentages automatically through the built-in software. The major components of the control bag and samples were Cl, C and O. In the sample bags Ca and P, and small traces of K, were also detected. In the "blue bag" sample, it is possible to notice an increase in the amount of chlorine, oxygen, magnesium and calcium, compared to the control one.

Table 2. Results of EDX analysis.

Element	Control (abs)	"Blue Bags" (abs)	Control Wt [Error] (%)	"Blue Bag" Wt [Error] (%)
Chlorine	25.25	33.34	16.63 [2.64]	25.17 [3.47]
Carbon	97.15	57.12	63.98 [32.64]	43.13 [20.96]
Oxygen	28.01	37.32	18.45 [10.09]	28.18 [13.12]
Sodium	-	1.91	-	1.44 [0.46]
Calcium	0.03	0.23	0.02 [0.08]	0.18 [0.10]
Potassium	-	0.08	-	0.06 [0.08]
Nickel	0.02	0.03	0.02 [0.08]	0.02 [0.08]
Aluminum	0.43	0.71	0.28 [0.14]	0.54 [0.18]
Magnesium	0.66	1.09	0.44 [0.19]	0.82 [0.26]
Phosphorus	-	0.19	-	0.14 [0.10]
Silicon	0.16	0.30	0.10 [0.10]	0.13 [0.12]
Neodymium	0.13	0.12	0.08 [0.09]	0.09 [0.09]

In particular, SEM + EDX analysis, performed on urine bags, before and after the presence of urine, showed an increase of ~32% of Cl, ~33% of O, ~667% of Ca, ~65% of Al and Mg, while C decreased by about 41%. Traces of P, Na, and K were found in the analyzed urine bag. They were probably present in the urine and deposited on the square sample of the "blue" bag surface. No variation was observed for Ni and Silicon.

4. Discussion

RS was described as a relevant technique for the analysis of biological materials of clinical interest. Since Raman spectrum is composed of sharp bands with distinct characteristics, specific for each molecule, a substance can be easily distinguished from the others due to the intrinsic biochemistry difference [28–30].

RS can be applied to the analysis of discolored urine, a phenomenon that can be observed in urine bags of hospitalized and long-term bedridden patients. A spectrum of urine colors (white, black, brown, red, pink, orange, yellow, blue-green, and purple) can occur due to changes in urochrome concentration and the presence of other pigments and both endogenous ones, such as uric acid, bilirubin, hemoglobin, or myoglobin, and exogenous causes related to patient diet, medications, and poisons.

As can be seen from an inspection of Figure 1, Raman spectra of urine from the bag show the presence of tryptophan (TRP) (1360 cm^{-1}) [31]. The TRP is sensitive to the microenvironment and detailed information about the microenvironment of these aromatic side chains can be obtained from variations in intensity of the vibrational modes [9]. The Raman spectrum also revealed the presence of indigo, a metabolite of TRP. TRP is an essential alpha-amino acid found in some foods, especially those high in protein (milk, meat, fish, beans, soybean, eggs, and others). It is needed for the in vivo biosynthesis of proteins and serves as a substrate for several bioactive metabolites, including serotonin, nicotinamide (vitamin B6), tryptamine, and others. In humans, TRP is exclusively obtained from dietary intake [32]. As detailed in Figure 3, the metabolic steps of TRP occur in the large intestine and liver up to the production of indoxyl sulphate (indican), a colorless product that is excreted in the urine tract. In patients, chronically catheterized and chair/bed-bound due to significant disability, like our patient, chronic constipation occurs typically, which causes increased indican excretion in the urinary tract, and, in turn, indigo presence.

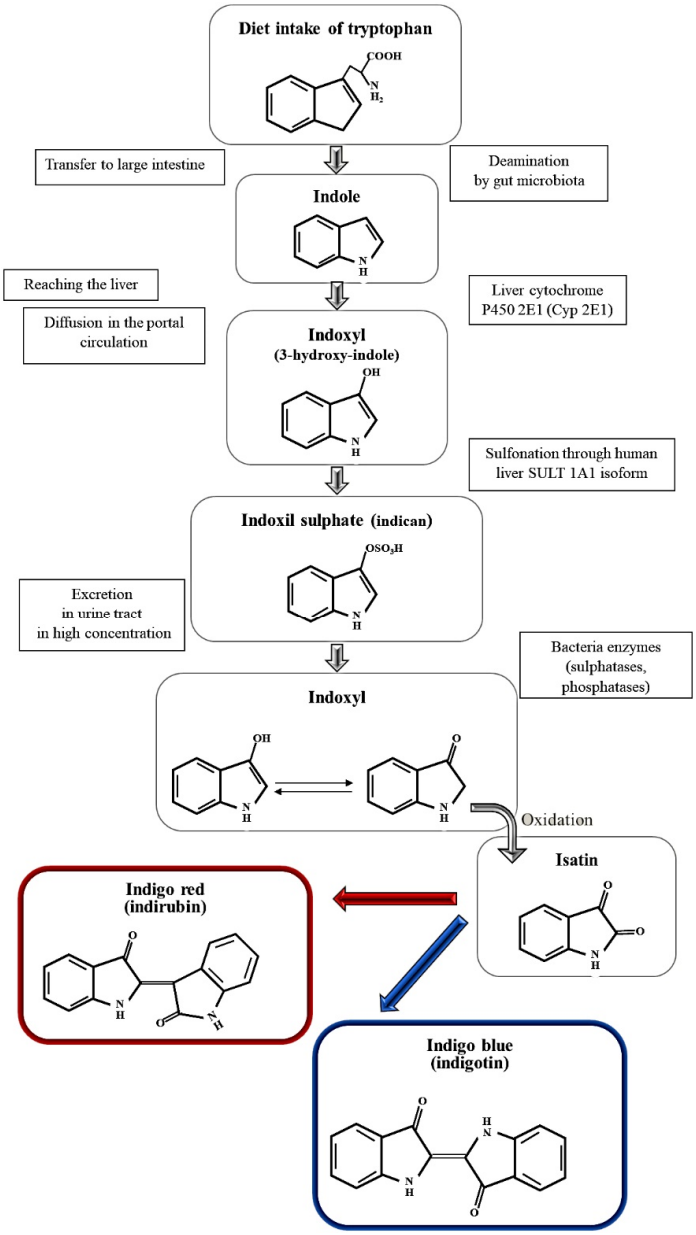

Figure 3. Metabolic steps of tryptophan (TRP).

In the presence of bacterial enzymes such as sulphatases and phosphatases, indican forms two isomeric metabolites: indigo blue (indigotin) and indigo red (indirubin). These metabolites dissolve in or deposit on the surface of urine bag material and are responsible for its blue/purple coloring according to the indigotin/indirubin ratio due to oxidative conditions and the pH value of the urine [33–35]. We found in the patient's urine both Gram+ and Gram− bacteria, which produce several types of enzymes, including sulphatases, phosphatases, catalase, and oxidase, capable of sticking to the urine bag surface, and growing and building a matrix to form a community named "biofilm" [36]. The image obtained under SEM showed that the urine bag had a wrinkled and rough surface, so we hypothesized the presence of microbial biofilm [37], which can be responsible for the variation of element values, perhaps because it represents an obstacle to correct scanning of the urine bag's surface.

Furthermore, the enzymatic features of microorganisms that we found in the patient's urine can at least partially explain the results obtained from EDX analysis, such as the presence of phosphorus and oxygen increase in the patient's urine with respect to the control one. The action of bacterial enzymes could also be applied to urine bag material consisting mainly of PVC.

5. Conclusions

The focus of the present study was to physically characterize the urine and urine bags to better understand the metabolic changes occurring in PUBS by using different techniques such as RS and SEM + EDX analysis, since no studies of such type were found in the literature. This study, based on just a single case, has to be intended as a proof-of-principle study, since it needs a wider number of cases to be studied to obtain a minimum statistical significance. Anyway, it can indicate an alternative approach to the treatment in the presence of PUBS.

RS revealed the presence of indigo, a metabolite of TRP, responsible for the typical apparent blue discoloration of urine. The biomarker presented different peaks representative of the different molecular vibrations.

SEM analysis showed the differences in morphological images between the control bag and sample ones, probably due to the presence of bacterial biofilm on the latter bag surface. The EDX technique revealed a predominant variation in the concentration of chlorine, oxygen, magnesium, and calcium, probably at least in part due to the action of bacterial enzymes.

The obtained morphological and analytical results provided us information of qualitative and quantitative modification in PUBS metabolite concentration with respect to the control. Thus, we intend to study a wider number of cases with the same methodology and techniques, so that we can reach at least a minimum level of statistical significance to eventually confirm validity of this procedure. Once statistically validated, we hope it can be used as an additional tool in the medical field for monitoring the evolution of PUBS for early detection of the presence of indigo in chronically catheterized and chair/bed-bound patients.

Supplementary Materials: The following supporting information can be downloaded at: https://www.mdpi.com/article/10.3390/app12084034/s1, Table S1: Comprehensive patient's medical history; Table S2: Clinical data of the patient.

Author Contributions: Conceptualization, C.S. and F.M.S.; Data curation, C.S., F.M.S. and B.T.; Formal analysis, M.R. and B.T.; Investigation, E.V.R.; Methodology, G.A. and B.T.; Resources, L.D.; Writing—original draft, G.A., C.S., F.M.S. and B.T.; Writing—review and editing, C.S. and F.M.S. All authors have read and agreed to the published version of the manuscript.

Funding: This research received no external funding.

Institutional Review Board Statement: The study did not require ethical approval.

Informed Consent Statement: The authors declare that no experiments have been conducted on animals and/or humans for this study. The study was conducted in accordance with the principles of the Declaration of Helsinki and in accordance with local statutory requirements. The authors declare that patient data do not appear in this article. The patient could understand the study design and objectives. Before participating in our study, the patient signed an informed consent form allowing us to use her biological fluids to publish this paper.

Acknowledgments: The authors wish to thank and honor the memory of Cetty Miuccio, thanks to whom it was possible to carry out this work.

Conflicts of Interest: The authors declare no conflict of interest.

References

1. Yang, H.W.; Su, Y.J. Trends in the epidemiology of purple urine bag syndrome: A systematic review. *Biomed. Rep.* **2018**, *8*, 249–256. [CrossRef] [PubMed]
2. Aycock, R. A Case of Purple Urine Bag Syndrome in a Patient with an Ileal Conduit. *Int. J. Nephrol. Urol.* **2010**, *2*, 580–583.
3. Al-Sardar, H.; Haroon, D. Purple urinary bag syndrome. *Am. J. Med.* **2009**, *122*, e1–e2. [CrossRef] [PubMed]
4. Peters, P.; Merlo, J.; Beech, N.; Giles, C.; Boon, B.; Parker, B.; Dancer, C.; Munckhof, W.; Teng, H.S. The purple urine bag syndrome: A visually striking side effect of a highly alkaline urinary tract infection. *Can. Urol. Assoc. J.* **2011**, *5*, 233–234. [CrossRef]
5. Wattanapisit, S.; Wattanapisit, A.; Meepuakmak, A.; Rakkapan, P. Purple urine bag syndrome in palliative care. *BMJ Support. Palliat. Care.* **2019**, *9*, 155–157. [CrossRef]
6. Worku, D.A. Purple urine bag syndrome: An unusual but important manifestation of urinary tract infection. Case report and literature review. *SAGE Open Med. Case Rep.* **2019**, *7*, 1–4. [CrossRef]
7. Austin, L.A.; Osseiran, S.; Evans, C.L. Raman technologies in cancer diagnostics. *Analyst* **2016**, *141*, 476–503. [CrossRef] [PubMed]
8. De Gaetano, F.; Cristiano, M.C.; Venuti, V.; Crupi, V.; Majolino, D.; Paladini, G.; Acri, G.; Testagrossa, B.; Irrera, A.; Paolino, D.; et al. Rutin-Loaded Solid Lipid Nanoparticles: Characterization and In Vitro Evaluation. *Molecules* **2021**, *26*, 1039. [CrossRef]
9. Giannetto, C.; Acri, G.; Giudice, E.; Arfuso, F.; Testagrossa, B.; Piccione, G. Quantifying serum total lipids and tryptophan cocentrations by Raman spectroscopy during standardized obstacle course in horses. *J. Equine Vet. Sci.* **2021**, *108*, 103820. [CrossRef]
10. Ye, K.; Li, K.; Lu, Y.; Guo, Z.; Ni, N.; Liu, H.; Huang, Y.; Ji, H.; Wang, P. An overview of advanced methods for the characterization of oxygen vacancies in materials. *TrAC Trends Anal. Chem.* **2019**, *116*, 102–108. [CrossRef]
11. Wang, Y.; Chen, D.; Zhang, J.; Balogun, M.-S.; Wang, P.; Tong, Y.; Huang, Y. Charge Relays via Dual Carbon-Actions on Nanostructured BiVO 4 for High Performance Photoelectrochemical Water Splitting. *Adv. Funct. Mater.* **2022**, *32*, 2112738. [CrossRef]
12. Langer, J.; Jimenez de Aberasturi, D.; Aizpurua, J.; Alvarez-Puebla, R.A.; Auguié, B.; Baumberg, J.J.; Bazan, G.C.; Bell, S.E.J.; Boisen, A.; Brolo, A.G.; et al. Present and Future of Surface-Enhanced Raman Scattering. *ACS Nano* **2020**, *14*, 28–117. [CrossRef] [PubMed]
13. Pilot, R.; Signorini, R.; Durante, C.; Orian, L.; Bhamidipati, M.; Fabris, L. A Review on Surface-Enhanced Raman Scattering. *Biosensors* **2019**, *9*, 57. [CrossRef] [PubMed]
14. Zhang, Y.; Mi, X.; Tan, X.; Xiang, R. Recent Progress on Liquid Biopsy Analysis using Surface-Enhanced Raman Spectroscopy. *Theranostics* **2019**, *9*, 491–525. [CrossRef]
15. Acri, G.; Romano, C.; Costa, S.; Pellegrino, S.; Testagrossa, B. Raman Spectroscopy Technique: A Non-Invasive Tool in Celiac Disease Diagnosis. *Diagnostics* **2021**, *11*, 1277. [CrossRef]
16. Saatkamp, C.J.; De Almeida, M.L.; Bispo, J.A.M.; Pinheiro, A.L.B.; Fernandes, A.B.; Silveira, L. Quantifying creatinine and urea in human urine through Raman spectroscopy aiming at diagnosis of kidney disease. *J. Biomed. Opt.* **2016**, *21*, 037001. [CrossRef]
17. Leal, L.B.; Nogueira, M.S.; Canevari, R.A.; Carvalho, L.F.C.S. Vibration spectroscopy and body biofluids: Literature review for clinical applications. *Photodiagnosis Photodyn. Ther.* **2018**, *24*, 237–244. [CrossRef]
18. Kušnír, J.; Dubayová, K.; Lešková, L.; Lajtár, M. Concentration matrices-solutions for fluorescence definition of urine. *Anal. Lett.* **2005**, *38*, 1559–1567. [CrossRef]
19. Saude, E.J.; Adamko, D.; Rowe, B.H.; Marrie, T.; Sykes, B.D. Variation of metabolites in normal human urine. *Metabolomics* **2007**, *3*, 439–451. [CrossRef]
20. Moreira, L.P.; Silveira, L.; Pacheco, M.T.T.; da Silva, A.G.; Rocco, D.D.F.M. Detecting urine metabolites related to training performance in swimming athletes by means of Raman spectroscopy and principal component analysis. *J. Photochem. Photobiol. B: Biol.* **2018**, *185*, 223–234. [CrossRef]
21. Bispo, J.A.M.; De Sousa Vieira, E.E.; Silveira, L.; Fernandes, A.B. Correlating the amount of urea, creatinine, and glucose in urine from patients with diabetes mellitus and hypertension with the risk of developing renal lesions by means of Raman spectroscopy and principal component analysis. *J. Biomed. Opt.* **2013**, *18*, 087004. [CrossRef] [PubMed]
22. Acri, G.; Testagrossa, B.; Faenza, P.; Caridi, F. Spectroscopic analysis of pigments of the Antonello Gagini annunciation's sculptural marble group, church of st. Theodore martyr (Bagaladi, Reggio Calabria, Italy): Case study. *Mediterr. Archaeol. Archaeom.* **2020**, *20*, 1–5. [CrossRef]

23. Meduri, A.; Severo, A.A.; De Maria, A.; Perroni, P.; Acri, G.; Testagrossa, B.; Puzzolo, D.; Montalbano, G.; Aragona, P.; Micali, A.G. PMMA intraocular lenses changes after treatment with Nd:Yag Laser: A scanning electron microscopy and X-ray spectrometry study. *Appl. Sci.* **2020**, *10*, 6321. [CrossRef]
24. Mijangos, F.; Celaya, M.A.; Gainza, F.J.; Imaz, A.; Arana, E. SEM-EDX linear scanning: A new tool for morpho-compositional analysis of growth bands in urinary stones. *J. Biol. Inorg. Chem.* **2020**, *25*, 705–715. [CrossRef]
25. Khan, M.S.I.; Oh, S.W.; Kim, Y.J. Power of Scanning Electron Microscopy and Energy Dispersive X-Ray Analysis in Rapid Microbial Detection and Identification at the Single Cell Level. *Sci. Rep.* **2020**, *10*, 2368. [CrossRef]
26. Goldsmith, C.S.; Miller, S.E. Modern uses of electron microscopy for detection of viruses. *Clin. Microbiol. Rev.* **2009**, *22*, 552–563. [CrossRef]
27. Tatsch, E.; Schrader, B. Near-infrared Fourier Transform Raman spectroscopy of indigoids. *J. Raman Spectrosc.* **1995**, *26*, 467–473. [CrossRef]
28. Acri, G.; Venuti, V.; Costa, S.; Testagrossa, B.; Pellegrino, S.; Crupi, V.; Majolino, D. Raman Spectroscopy as Noninvasive Method of Diagnosis of Pediatric Onset Inflammatory Bowel Disease. *Appl. Sci.* **2020**, *10*, 6974. [CrossRef]
29. Silveira, L.J.; de Cassia Fernandes Borges, R.; Navarro, R.S.; Giana, H.E.; Zangaro, R.A.; Pacheco, M.T.T.; Fernandes, A.B. Quantifying glucose and lipid components in human serum by Raman spectroscopy and multivariate statistc. *Laseres Med. Sci.* **2017**, *32*, 787–795. [CrossRef]
30. Acri, G.; Micali, A.; D'Angelo, R.; Puzzolo, D.; Aragona, P.; Testagrossa, B.; Aragona, E.; Wylegala, E.; Nowinska, A. Raman Spectroscopic Study of Amyloid Deposits in Gelatinous Drop-like Corneal Dystrophy. *J. Clin. Med.* **2022**, *11*, 1403. [CrossRef]
31. Rygula, A.; Majzner, K.; Marzec, K.M.; Kaczor, A.; Pilarczyk, M.; Baranska, M. Raman spectroscopy of proteins: A review. *J. Raman Spectrosc.* **2013**, *44*, 1061. [CrossRef]
32. Friedman, M. Analysis, Nutrition, and Health Benefits of Tryptophan. *Int. J. Tryptophan Res.* **2018**, *11*, 1–12. [CrossRef] [PubMed]
33. Barlow, G.B.; Dickson, J.A.S. Purple urine bags. *Lancet* **1978**, *311*, 220–221. [CrossRef]
34. Dealler, S.F.; Hawkey, P.M.; Millar, M.R. Enzymatic degradation of urinary indoxyl sulfate by Providencia stuartii and Klebsiella pneumoniae causes the purple urine bag syndrome. *J. Clin. Microbiol.* **1988**, *26*, 2152–2156. [CrossRef]
35. Dealler, S.F.; Belfield, P.W.; Bedford, M.; Whitley, A.J.; Mulley, G.P. Purple urine bags. *J. Urol.* **1989**, *142*, 769–770. [CrossRef]
36. Willett, J.L.E.; Ji, M.M.; Dunny, G.M. Exploiting biofilm phenotypes for functional characterization of hypothetical genes in Enterococcus faecalis. *NPJ Biofilms Microbiomes* **2019**, *5*, 23. [CrossRef]
37. Lee, K.H.; Park, S.J.; Choi, S.; Uh, Y.; Park, J.Y.; Han, K.-H. The Influence of Urinary Catheter Materials on Forming Biofilms of Microorganisms. *J. Bacteriol. Virol.* **2017**, *47*, 32–40. [CrossRef]